Engineering Structures 133 (2017) 124–132

Contents lists available at ScienceDirect

Engineering Structures

journal homepage: www.elsevier.com/locate/engstruct

Effect of pavement maintenance cycle on the fatigue reliability of simply-supported steel I-girder bridges under dynamic vehicle loading

Lu Deng [a], Wei Wang [a,*], C.S. Cai [b]

[a] Key Laboratory for Wind and Bridge Engineering of Hunan Province, Hunan University, Changsha, Hunan 410082, China
[b] Dept. of Civil and Environmental Engineering, Louisiana State University, Baton Rouge, LA 70803, United States

ARTICLE INFO

Article history:
Received 18 April 2016
Revised 16 October 2016
Accepted 13 December 2016

Keywords:
Pavement maintenance cycle
Steel I-girder bridge
Road surface condition
Deterioration process
Reliability analysis

ABSTRACT

In this study, the effect of the pavement maintenance cycle on the fatigue reliability of simply-supported steel I-girder bridges under dynamic vehicle loading is studied. The bridge model and the fatigue load model are both adopted from the Load and Resistance Factor Design (LRFD) Bridge Design Specifications of the American Association of State Highways and Transportation Officials (AASHTO). A three-dimensional vehicle-bridge coupled model is developed to simulate the vehicle-bridge interaction and used to obtain the stress ranges of the steel bridge girders under the dynamic vehicle loading. Numerical simulations are carried out to study the influence of three important parameters, including the road surface condition, bridge span length and vehicle speed, on the fatigue damage induced by the fatigue truck. The results from this study show that the bridge fatigue reliability decreases dramatically under repeated dynamic vehicle loads when the road surface condition is very poor and that the pavement maintenance cycle has a significant influence on the bridge fatigue reliability. A procedure for determining the desired pavement maintenance cycle to achieve the target fatigue reliability of steel bridge girders is developed. An example is also provided for demonstrating the proposed procedure.

1. Introduction

Vehicle-induced fatigue problem is one of the main issues that need to be considered in the design and assessment of steel bridges. With the ever-increasing traffic on highways, the fatigue problem of steel bridges has received more and more attention.

The fatigue design of steel bridges is usually based on the static stress under the fatigue vehicle loads and uses a fatigue impact factor to account for the dynamic load effects. For example, the Load and Resistance Factor Design (LRFD) Bridge Design Specification of the American Association of State Highways and Transportation Officials (AASHTO) adopts an impact factor of 0.15 for fatigue design [1]. However, recent studies found that the vehicle dynamic effect may have been underestimated when analyzing the fatigue of steel bridges, especially under deteriorated road surface conditions (RSCs) which can lead to very large dynamic vehicle loads [2]. Zhang and Cai [2,3] studied the fatigue reliability of a steel bridge based on the concept of equivalent fatigue damage and found that the fatigue reliability of bridge components is greatly affected by the road surface deterioration rate.

Maintaining the road surface in good conditions can reduce the dynamic effect of vehicle loads and therefore the stress ranges of bridge components, leading to increased fatigue life and fatigue reliability of the bridge components. The pavement maintenance plan of bridges was usually determined based on a life-cycle cost analysis approach [4–9] and most of these studies were focused on the cost and the reliability of the pavement [10–12]. Little attention has been paid to the fatigue problem of the bridge components. Therefore, this study aims to reveal the influence of pavement maintenance cycle on the fatigue reliability of bridge girders and to provide suggestions for the decision-making on pavement maintenance plan from this point view.

In this paper, a three-dimensional vehicle-bridge coupled model was developed to simulate the bridge responses under the dynamic vehicle loading. The bridge stresses were obtained from the numerical simulations using the vehicle-bridge coupled model. Based on the numerical simulation results, the effects of the road surface condition and the pavement maintenance cycle on the fatigue reliability of simply-supported steel I-girder bridges under dynamic vehicle loading were studied. A procedure for determining the desired pavement maintenance cycle to achieve the target fatigue reliability of steel bridge girders was developed. An example was also provided for demonstrating the proposed procedure.

* Corresponding author at: Key Laboratory for Wind and Bridge Engineering of Hunan Province, Hunan University, Changsha, Hunan 410082, China.

E-mail address: wangwei190104@gmail.com (W. Wang).

http://dx.doi.org/10.1016/j.engstruct.2016.12.022
0141-0296/

2. Analytical bridge

Simply-supported steel I-girder bridges constitute a major proportion of steel bridges in the United States. In this study, five simply-supported steel I-girder bridges with common span lengths ranging from 10.67 m (35 ft) to 36.58 m (120 ft) were designed following the AASHTO LRFD Bridge Design Specifications [1]. Each bridge has five identical girders spaced at 2.13 m (7 ft) and has a roadway width of 9.75 m (32 ft) and a bridge deck thickness of 0.20 m (8 in.). The cross-section of Bridge 2 was taken as an example for illustration and is shown in Fig. 1. In addition to the end diaphragms used for all five bridges, intermediate diaphragms were used for bridges with relative long spans. Fig. 2 shows the finite element model of Bridge 2 created using the ANSYS 14.5 program [13]. Some basic parameters and the fundamental frequencies of the five bridges are summarized in Table 1.

3. Truck model

The AASHTO LRFD Bridge Design Specifications [1] specifies a fatigue truck model with detailed sizes and weight to be used in bridge fatigue design. An analytical model of this truck is shown in Fig. 3. A summary of the basic parameters of the truck, including the geometry, mass distribution, damping, and stiffness of the tires and suspension systems, are shown in Table 2 [14]. The size and weight of this truck were derived based on surveyed truck data [15] and can well represent the equivalent fatigue damage accumulation caused by the truck traffic which consists of trucks with a variety of gross vehicle weights and axle configurations [16]. Therefore, this truck model was used in the analysis of this study.

4. Vehicle-bridge coupled system for numerical simulations

4.1. Dynamic equation of the vehicle

The dynamic response of a vehicle can be obtained by solving the equation of motion as follows:

$$[M_v]\{\ddot{d}_v\} + [C_v]\{\dot{d}_v\} + [K_v]\{d_v\} = \{F_G\} + \{F_v\} \tag{1}$$

where $[M_v]$, $[C_v]$, and $[K_v]$ = the vehicle's mass, damping, and stiffness matrices, respectively; $\{d_v\}$ = the vector of the vehicle's displacement; $\{F_G\}$ = the vector of the vehicle's gravity; and $\{F_v\}$ = the vector of wheel-road interaction forces acting on the vehicle.

4.2. Dynamic equation of the bridge

The dynamic equation of a bridge can be written as follows:

$$[M_b]\{\ddot{d}_b\} + [C_b]\{\dot{d}_b\} + [K_b]\{d_b\} = \{F_b\} \tag{2}$$

where $[M_b]$, $[C_b]$, and $[K_b]$ = the bridge's mass, damping, and stiffness matrices, respectively; $\{d_b\}$ = the bridge's displacement vector; and $\{F_b\}$ = the vector of wheel-road interaction forces that are applied to the bridge.

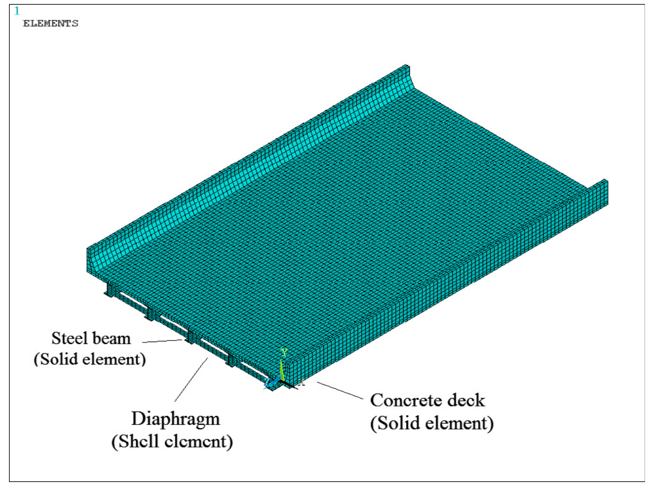

Fig. 2. Finite element model of Bridge 2.

4.3. Establishing the vehicle-bridge coupled system

The interaction forces between the bridge and vehicle are force and reaction forces which are equal in magnitude but with opposite directions. At the contacting points, the displacement of the bridge, the displacement of the wheel axle, the deformation of the tire spring and the road roughness are compatible [17]. Based on these two relationships, a coupled equation for the vehicle-bridge system can be established by combining Eqs. (1) and (2), as shown below:

$$\begin{bmatrix} M_b & \\ & M_v \end{bmatrix} \begin{Bmatrix} \ddot{d}_b \\ \ddot{d}_v \end{Bmatrix} + \begin{bmatrix} C_b + C_{bb} & C_{bv} \\ C_{vb} & C_v \end{bmatrix} \begin{Bmatrix} \dot{d}_b \\ \dot{d}_v \end{Bmatrix} + \begin{bmatrix} K_b + K_{bb} & K_{bv} \\ K_{vb} & K_v \end{bmatrix} \begin{Bmatrix} d_b \\ d_v \end{Bmatrix} = \begin{Bmatrix} F_{br} \\ F_{vr} + F_G \end{Bmatrix} \tag{3}$$

where C_{bb}, C_{bv}, C_{vb}, K_{bb}, K_{bv}, K_{vb} are the damping and stiffness terms related the interaction between the bridge and vehicle; F_{br} and $F_{vr}$are due to the contact force between the bridge and the vehicle and are also time-dependent terms [18].

The sizes of the matrices in Eq. (3) can be reduced by adopting the modal superposition technique, which transforms Eq. (3) to the following simplified equation:

$$\begin{bmatrix} I & \\ & M_v \end{bmatrix} \begin{Bmatrix} \ddot{\xi}_b \\ \ddot{d}_v \end{Bmatrix} + \begin{bmatrix} 2\omega_i\eta_i I + \Phi_b^T C_{bb}\Phi_b & \Phi_b^T C_{bv} \\ C_{vb}\Phi_b & C_v \end{bmatrix} \begin{Bmatrix} \dot{\xi}_b \\ \dot{d}_v \end{Bmatrix} + \begin{bmatrix} \omega_i^2 I + \Phi_b^T K_{bb}\Phi_b & \Phi_b^T K_{bv} \\ K_{vb}\Phi_b & K_v \end{bmatrix} \begin{Bmatrix} \xi_b \\ d_v \end{Bmatrix} = \begin{Bmatrix} \Phi_b^T F_{br} \\ F_{vr} + F_G \end{Bmatrix} \tag{4}$$

The vehicle-bridge coupled system in Eq. (4) was then solved using the fourth-order Runge-Kutta method in the time domain in the Matlab environment. More details about the establishment of the bridge-vehicle coupled system and the solutions can be found in [17,18] and are therefore not provided in this paper.

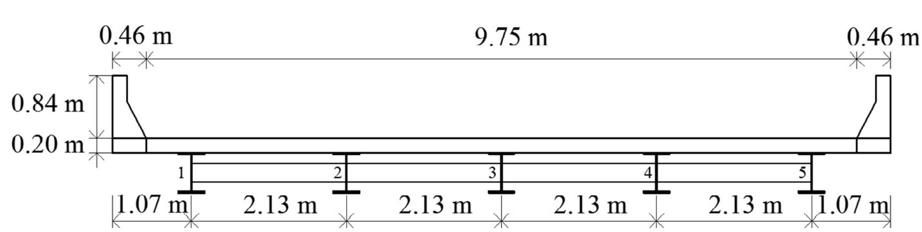

Fig. 1. Cross-section of Bridge 2.

Table 1
Detailed properties of the five studied bridges.

Bridge number	Span length (m)	Girder		Number of intermediate diaphragm	Fundamental frequency (Hz)
		Cross-sectional area (m^2)	Inertia moment of cross-section (10^{-2} m^4)		
1	10.67	0.018	0.040	1	12.40
2	16.76	0.020	0.109	2	8.62
3	22.86	0.023	0.219	2	6.10
4	30.48	0.026	0.421	3	4.39
5	36.58	0.028	0.641	4	3.49

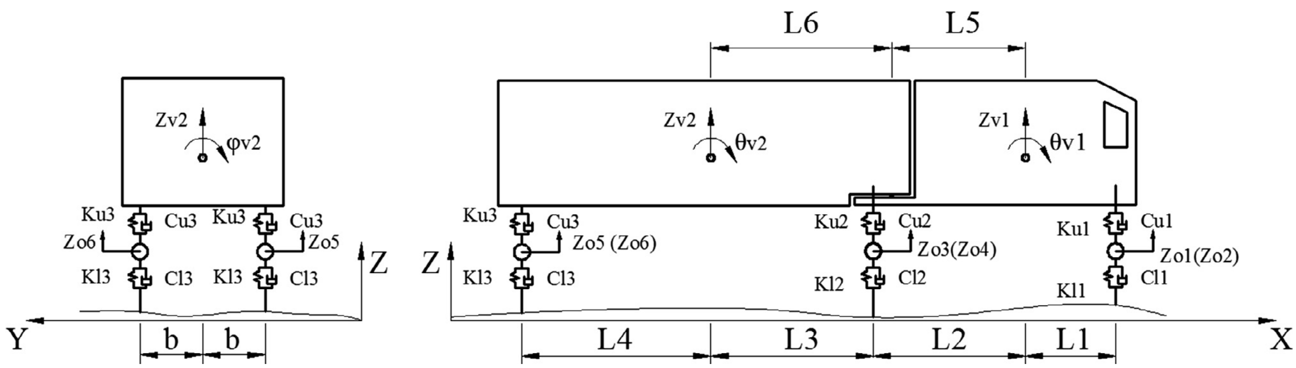

Fig. 3. Analytical model of the adopted truck.

Table 2
Main parameters of the HS20-44 truck model adopted in this study.

Items	Parameters	Values
Mass	Truck body 1	2612 (kg)
	Truck body 2	26,113 (kg)
	First axle suspension	490 (kg)
	Second axle suspension	808 (kg)
	Third axle suspension	653 (kg)
Geometry	L1	1.698 (m)
	L2	2.569 (m)
	L3	4.452 (m)
	L4	4.692 (m)
	L5	2.215 (m)
	L6	4.806 (m)
	b	1.1 (m)
Moment of inertia	Pitching, truck body 1	2022 (kg m^2)
	Rolling, tuck body 1	8544 (kg $m^{2)}$
	Pitching, truck body 2	33,153 (kg m^2)
	Rolling, tuck body 2	181,216 (kg m^2)
Spring stiffness	Upper, first axle	242,604 (N/m)
	Lower, first axle	875,082 (N/m)
	Upper, second axle	1,903,172 (N/m)
	Lower, second axle	3,503,307 (N/m)
	Upper, third axle	1,969,034 (N/m)
	Lower, third axle	3,507,429 (N/m)
Damper coefficient	Upper, first axle	2190 (N s/m)
	Lower, first axle	2000 (N s/m)
	Upper, second axle	7882 (N s/m)
	Lower, second axle	2000 (N s/m)
	Upper, third axle	7182 (N s/m)
	Lower, third axle	2000 (N s/m)

The accuracy and reliability of the bridge-vehicle coupled system was also verified with a series of field tests in other research works of the authors [19,20]. The bridge responses obtained from the numerical simulation, including bridge deflections and strains at the mid-span of the girders, were compared and agreed well with the field measured results.

Once the bridge dynamic responses are solved, the stress can then be calculated with the following equation:

$$[S] = [E][B][d_b] \tag{5}$$

where [E] represents the matrix of the stress-strain relation; the elements of the matrix [E] are usually assumed to have constant values over each finite element of the bridge model; and [B]represents the matrix of the strain-displacement relation that is assembled with the x, y, and z derivatives of the element shape functions that can be derived following a standard finite element formulation procedure. The stress time histories of the steel girders obtained from numerical simulations using the coupled vehicle-bridge model were used in the fatigue analysis.

5. Deterioration model of the RSC

5.1. Generation of road surface profile

RSC plays a significant role in exciting the dynamic interaction between a bridge and passing vehicles. A road surface profile can usually be treated as a zero-mean stationary Gaussian random process. A random road surface profile can be generated by an inverse Fourier transformation of a power spectral density (PSD) function [21], as shown below:

$$r(X) = \sum_{k=1}^{N} \sqrt{2\varphi(n_k)\Delta n} \cos(2\pi n_k X + \theta_k) \tag{6}$$

where $\varphi()$ is the PSD function (m^3/cycle); θ_k is a random phase angle uniformly distributed from 0 to 2π; and n_k is the wave number (cycle/m). In the present study, the following PSD function [22] was adopted:

$$\varphi(n) = \varphi(n_0)\left(\frac{n}{n_0}\right)^{-2} \quad (n_1 < n < n_2) \tag{7}$$

where n_0 is the discontinuity frequency of $1/2\pi$ (cycle/m); $\varphi(n_0)$ is the roughness coefficient (m^3/cycle) whose value is chosen depending on the road condition; and n_1 and n_2 are the lower and upper cut-off frequencies, respectively.

Table 3
RRC values for different road-roughness classifications.

Road-roughness classification	Ranges for RRC (m^3/cycle)
Very good	2×10^{-6}–8×10^{-6}
Good	8×10^{-6}–32×10^{-6}
Average	32×10^{-6}–128×10^{-6}
Poor	128×10^{-6}–512×10^{-6}
Very poor	512×10^{-6}–2048×10^{-6}

The International Organization for Standardization [23] defines five road roughness classifications (denoted by j hereafter where $j = 1$, 2, 3, 4, and 5 representing very good, good, average, poor, and very poor RSCs, respectively) based on different ranges of the road-roughness coefficient (RRC) listed in Table 3. In this research the classification of road roughness based on the ISO [23] was used.

5.2. Progressive deterioration of RSC

Under the combined action of traffic loads and environmental corrosion, road pavement experiences progressive deterioration. To describe the progressive deterioration of the bridge RSC, the following model can be used [24]:

$$\varphi(n_0)_t = 6.1972 \times 10^{-9} \times \exp\{[1.04e^{\eta t} \cdot IRI_0 + 263(1 + SNC)^{-5}(CESAL)_t]/0.42808\} + 2 \times 10^{-6} \tag{8}$$

where $\varphi(n_0)_t$ is the road roughness coefficient as a function of time from the opening of the new road; IRI_0 is the initial roughness value before the road is opened to traffic; η is the environmental coefficient depending on the environmental condition and can vary from 0.01 to 0.7; t is the time in years; SNC is the structural number calculated based on the strength and thickness of each layer in the pavement; and $(CESAL)_t$ is the estimated number of traffic (in millions) in terms of the AASHTO equivalent single axle load of 80-kN (18-kip) at time t.

Bridges may experience rain and freezing conditions during their service life. By referring to the study of Shiyab [25], for bridges that are exposed in wet and freezing conditions (general condition), the SNC were calculated to be 6.19 and η was adopted as 0.1. Based on the AASHTO LRFD Bridge Design Specifications [1], the average daily truck traffic (ADTT) and the fraction of traffic in a single lane were taken as 2000 and 0.85, respectively, in this research for the purpose of illustration. Assuming no traffic increase, the $CESAL$ number was calculated to be 12.42 for each lane each year [25].

By substituting the values of SNC, $CESAL$ and η into Eq. (8), the time taken for the RSC to deteriorate from one class to the next can be calculated. The number of truck passages, denoted by N_{Tj} ($j = 1$, 2, 3, 4, 5), taken for the RSC to deteriorate from one class to the next was also obtained based on the assumed ADTT. For instance, N_{T1} represents the number of truck passages required for the RSC to deteriorate from the class "very good" to the class "good". A summary of the calculated time (t_j) and number of truck passages (N_{Tj}) needed for the RSC at each class to deteriorate to the next is shown in Table 4. The total time (T) taken for the RSC to deteriorate to the end of each class after being opened to traffic was also calculated. Table 4 shows that under the assumed traffic and environmental conditions, the pavement life cycle was calculated to be 12.60 years.

6. Numerical study

In this section, numerical simulations were performed for fatigue analysis using the developed bridge-vehicle coupled system. Many researchers have investigated the effect of important parameters on the bridge-vehicle interaction [26–28]. Based on the results from previous studies, three parameters were investigated in the present study, namely, RSC, bridge span length and vehicle speed.

As discussed previously, all five different RSCs defined by the ISO [23] were considered, namely, very good, good, average, poor and very poor. A total of seven vehicle speeds ranging from 30 km/h to 120 km/h were considered. The fatigue truck model and the loading position shown in Fig. 4, as specified by the AASHTO LRFD Bridge Design Specifications [1], were adopted in this study. Fig. 5 shows the maximum static stress at the mid-span position of all five girders of each bridge when one fatigue truck travels across the bridge with a very slow speed with the lateral position fixed as shown in Fig. 4. It can be seen that for all five bridges the maximum static stress occurs consistently at the mid-span of Girder 4. Therefore, the stresses of Girder 4 were used for fatigue analysis hereafter. The detail considered in the study was the connection point between the bottom flange and the web, which corresponds to Category B for welded joints as specified in the AASHTO LRFD Bridge Design Specifications [1].

Due to the fact that the randomly-generated road surface profile could bring bias to the results obtained, under each case with a

Table 4
The number of truck passages and time taken for the RSC to deteriorate to the next class.

Parameter	RSC				
	Very good	Good	Average	Poor	Very poor
N_{Tj}	4,113,464	1,156,504	938,321	839,119	768,396
t_j (years)	6.63	1.86	1.52	1.35	1.24
T (years)	6.63	8.49	10.01	11.36	12.60

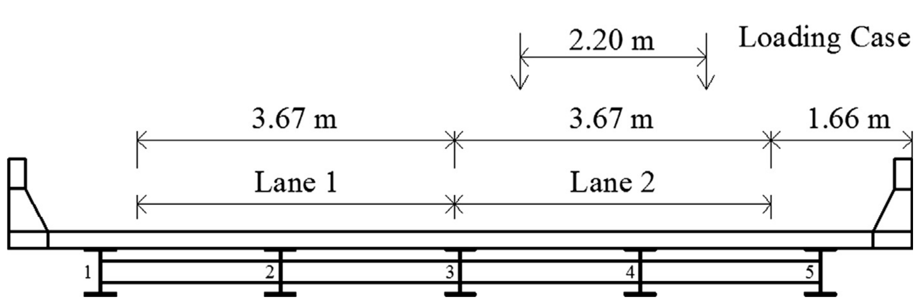

Fig. 4. The vehicle loading position adopted in the study.

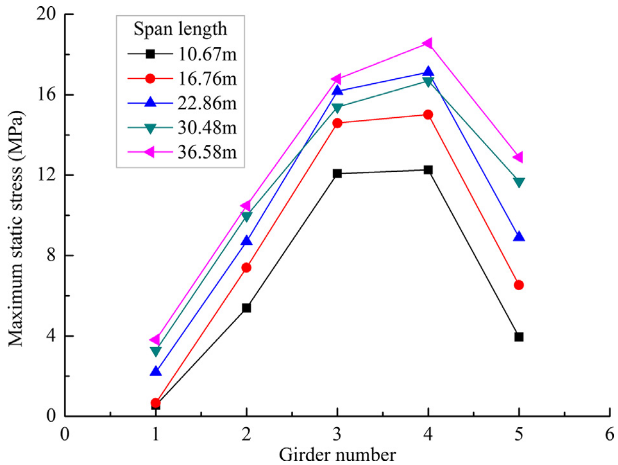

Fig. 5. Maximum static stresses at the mid-spans of the bridge under loading case considered.

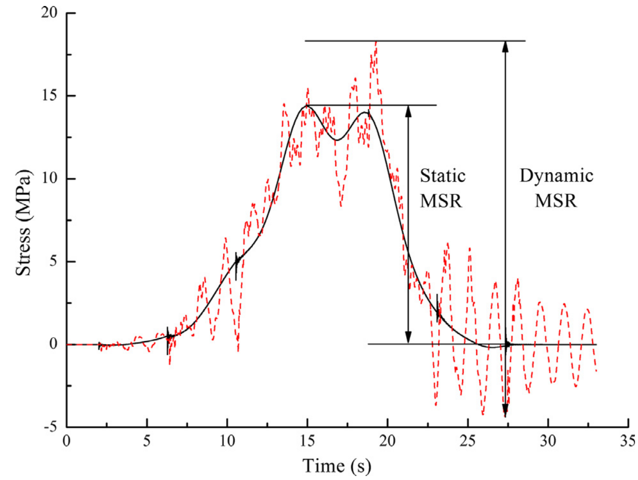

Fig. 6. Illustration of the maximum stress range.

given vehicle speed and RSC, the bridge-vehicle coupled analysis was repeated 20 times and 20 simulated results were obtained under the given RSC. By using 20 simulations, the coefficient of variation of the bridge stress results can be controlled under 10% [18], and a satisfactory convergence level could be achieved [27]. Then, the average values of the 20 simulations were used for fatigue analysis.

6.1. Expression of the FD

Bridge components will experience complex stress cycles under the action of passing trucks, leading to the accumulation of the FD. According to Miner's rule [29], the accumulated fatigue damage (AFD) can be estimated as:

$$AFD(t) = \sum_i \frac{n_i}{N_i} \tag{9}$$

where n_i is the number of cycles accumulated at a stress range level of S_i and N_i is the average number of cycles to failure at this stress level. It should be noted that Miner's rule [29] assumes linear damage accumulation and does not consider the effect of the order of stress [30,31]. Based on the fatigue analysis approach specified in the AASHTO LRFD Bridge Design Specifications [1], N_i and S_i satisfy the following relationship:

$$N_i = \frac{A}{S_i^m} \tag{10}$$

where A is the fatigue-strength coefficient and m is the slope constant which is usually taken as 3 for all AASHTO fatigue category details [32]. After substituting Eq. (10) into Eq. (9), the following equation can be obtained:

$$AFD(t) = \sum_i \frac{n_i S_i^3}{A} \tag{11}$$

Fig. 6 shows the typical static and dynamic stress time history curves of the target point of Bridge 2. The static stress curve (the solid line in Fig. 6) was obtained when the truck crossed the bridge with a very slow speed while the dynamic stress curve (the dashed line in Fig. 6) was obtained when the truck crossed the bridge under good RSC at a speed of 45 km/h. The algebraic difference between the maximum and minimum stresses is the maximum stress range (*MSR*), as illustrated in Fig. 6.

According to the study of Schilling [33], with the complex stress cycles induced by each truck passage, the cumulative fatigue damage can be calculated based on the primary or maximum stress range and the corresponding equivalent number of stress cycles (*ENSC*), which can be determined using the following equation:

$$ENSC = num + \left(\frac{S_{r1}}{MSR}\right)^m + \left(\frac{S_{r2}}{MSR}\right)^m + \cdots + \left(\frac{S_{ri}}{MSR}\right)^m + \cdots + \left(\frac{S_{rcut}}{MSR}\right)^m \tag{12}$$

where num = the number of maximum stress range caused by each truck passage; S_{ri} ($i = 1 \cdots cut$) = the higher-order stress ranges; and S_{rcut} = the cutoff stress range. In this study, the slope constant m was taken as 3 for the AASHTO fatigue category details [32], and the rainflow counting algorithm was used to extract the number of stress ranges from the stress history [34].

A reasonable cutoff value is necessary when calculating the *ENSC*, as can be seen from Eq. (12). According to previous studies, the upper limit for the cut-off stress range for welded details is usually set to 25–33% of the CAFL in previous studies [35,36] while the applicable stress range cut-off levels could range between 3.45 MPa (0.5 ksi) and 36.40 MPa (5.28 ksi) (33% of the CAFL) [37,38]. In this research, the cutoff stress range was set to 3.45 MPa (0.5 ksi), which could result in relatively conservative results.

It is known from Eq. (11) that the *AFD* is related to the summation of the cube of the stress range multiplied by its corresponding number of stress cycles. Therefore, the *FD* due to each truck passage under different RSCs, denoted by j ($j = 1, 2, 3, 4, 5$) as discussed previously, can be defined as follows:

$$FD_j = ENSC_j \cdot MSR_j^3 \tag{13}$$

Based on the numerical simulation results, Eqs. (12) and (13), the average *FD*s of 20 simulations under the action of the fatigue truck considered are plotted against vehicle speed in Fig. 7. Again, the average values of twenty simulations for each specific case were adopted in order to reduce the bias that may be brought into the results due to the randomly-generated road surface profile. From Fig. 7, it can be observed that the average *FD* is greatly affected by the RSC. For instance, the average *FD* of Bridge 1 increases from 2.41×10^3 MPa^3 when the RSC is very good to 1.20×10^6 MPa^3 when the RSC is very poor. However, the increase of vehicle speed does not necessarily lead to the increase of the *FD* due to the fact that increasing the vehicle speed does not necessarily intensify the bridge-vehicle interaction [27,39].

6.2. Distribution of the FD

The distribution of the *FD* of the bridge considered under different RSCs was needed in the fatigue reliability analysis. The

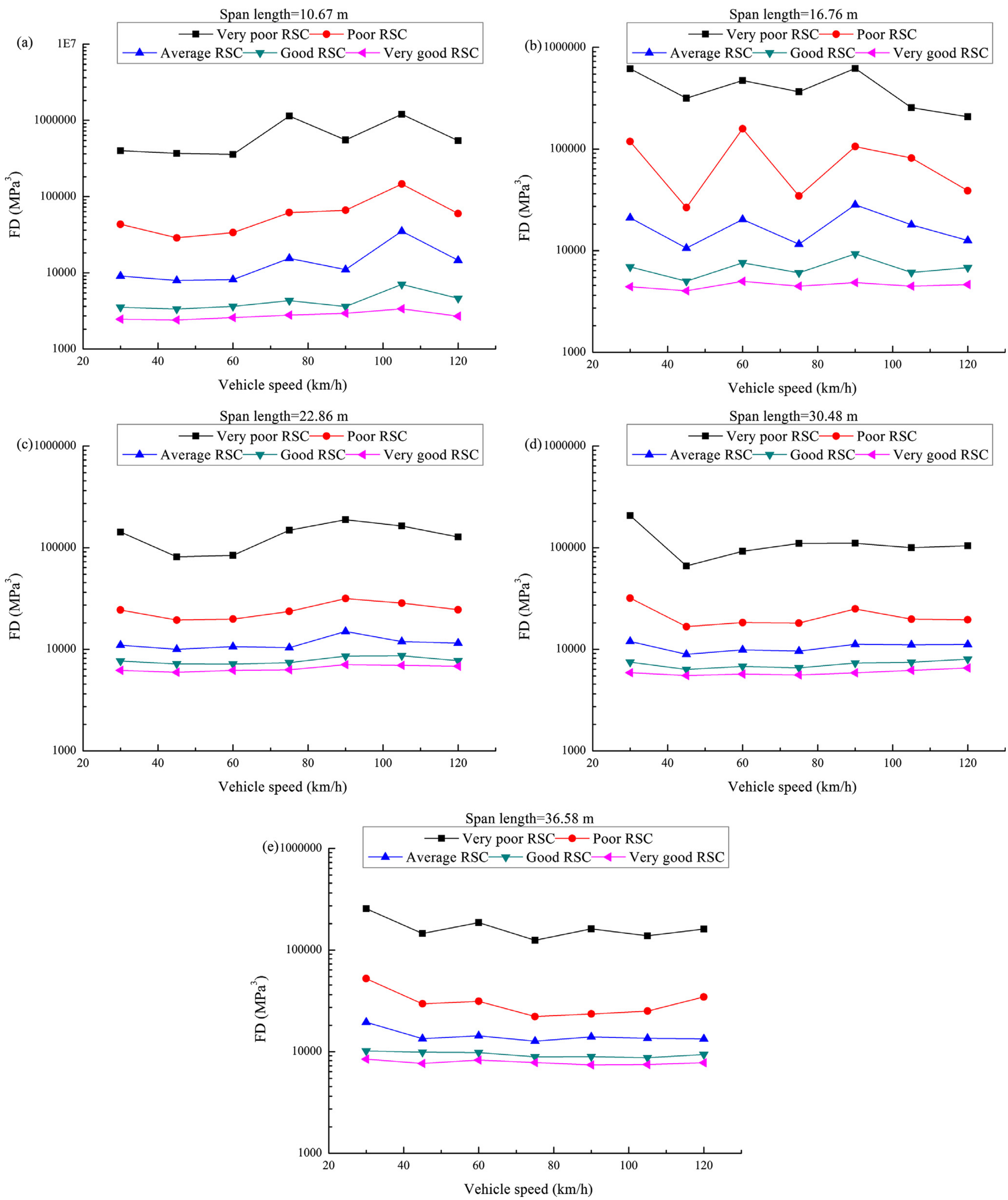

Fig. 7. Variation of the FD with change in vehicle speed and RSC for the bridge under the action of the truck considered.

Chi-square test was used to determine the distribution of the calculated 140 *FDs* (7 speeds × 20 replicates) for the bridge under each RSC. In the present study, the number of intervals of the histogram used in the Chi-square test was set to be 10 and the significance level was set to 0.99. As a result, the threshold value for the Chi-square test was determined to be 23.21.

The calculated *FDs* for the bridge under different RSCs were tested against two of the most common distribution types, namely, the normal and lognormal distributions. The test results are summarized in Table 5.

From Table 5 it can be observed that for the bridge considered the Chi-square test values for the lognormal distribution are all below the threshold value of 23.21 for each of the RSCs. However, a significant portion of the test values for the normal distribution are above the threshold value. These test results indicate that the log-normal distribution can be used to describe the *FD*s with significant confidence. The statistical properties of the *FD*s induced by truck passages under different RSCs are summarized in Table 6.

7. Effect of pavement maintenance cycle on the target fatigue reliability

According to a previous study in 2007 [40], 28% of the total 586,000 bridges in the United States were found deficient, and half of these bridges were structurally deficient. Poor road conditions can magnify the dynamic effect of vehicle loading and therefore lead to accelerated deterioration of bridge condition. On the other hand, well-maintained pavement can reduce the dynamic vehicle loading and therefore reduce the fatigue damage to the bridge components as well.

In this section, the effect of pavement maintenance cycle on the fatigue reliability of the bridge girders was studied and a procedure for determining the pavement maintenance cycle to achieve the target fatigue reliability of steel bridge girders is put forward. The goal was that with the minimum number of maintenance cycles the fatigue reliability of the bridge girders can satisfy the target reliability index during the 75-year service life.

The fatigue limit state function is defined as follows:

$$g(X) = \Delta - \mathrm{AFD}(t) \tag{14}$$

where Δ is the damage to cause fatigue failure and was found to follow a lognormal distribution with a mean value of 1.0 and a coefficient of variation of 0.3 [41], and g is a failure function. Fatigue failure occurs when "g < 0".

Assume N_p is the number of pavement maintenance, based on Eqs. (11) and (13), the *AFD* induced by truck passages under different RSCs after N_p pavement maintenance cycles can be calculated as:

$$AFD(t) = \frac{n_1 S_1^3}{A} + \frac{n_2 S_2^3}{A} + \cdots + \frac{n_5 S_5^3}{A} \tag{15}$$

Table 5
Chi-square test results on the distribution of FDs for each bridge under different RSCs.

Bridge number	RSC	Distribution type	
		Log-normal	Normal
1	Very good	6.82	14.51
	Good	12.44	58.66
	Average	5.25	194.84
	Poor	2.54	104.60
	Very poor	2.05	125.55
2	Very good	5.23	12.23
	Good	11.47	24.68
	Average	6.42	73.74
	Poor	6.53	177.87
	Very poor	3.63	64.75
3	Very good	9.41	13.79
	Good	5.49	16.21
	Average	5.25	20.13
	Poor	4.55	27.06
	Very poor	1.37	27.58
4	Very good	6.72	11.61
	Good	16.70	24.96
	Average	5.39	25.88
	Poor	6.63	32.29
	Very poor	3.29	45.84
5	Very good	2.43	3.49
	Good	2.71	8.15
	Average	4.58	21.34
	Poor	5.17	54.66
	Very poor	3.46	30.99

Table 6
Statistical properties of the *FD*s induced by truck passages under different RSCs.

Bridge number	RSC	Mean (MPa^3)	COV
1	Very good	2.75×10^3	0.21
	Good	4.30×10^3	0.52
	Average	1.15×10^4	0.29
	Poor	6.28×10^4	1.10
	Very poor	6.53×10^5	1.25
2	Very good	4.55×10^3	0.16
	Good	6.83×10^3	0.33
	Average	1.75×10^4	0.79
	Poor	8.05×10^4	1.42
	Very poor	4.08×10^5	0.96
3	Very good	6.49×10^3	0.10
	Good	7.76×10^3	0.17
	Average	1.15×10^4	0.29
	Poor	2.45×10^4	0.52
	Very poor	1.34×10^5	0.57
4	Very good	5.90×10^3	0.09
	Good	7.13×10^3	0.15
	Average	1.05×10^4	0.26
	Poor	2.13×10^4	0.45
	Very poor	1.13×10^5	0.70
5	Very good	7.83×10^3	0.09
	Good	9.39×10^3	0.16
	Average	1.44×10^4	0.35
	Poor	8.05×10^4	1.42
	Very poor	1.67×10^5	0.60

In Eq. (15), $n_j S_j^3 = N_p \cdot N_{Tj} \cdot ENSC_j \cdot MSR_j^3 = N_p \cdot N_{Tj} \cdot FD_j$ ($j = 1$, 2, 3, 4, 5), and N_{Tj} is the number of truck passages taken for the RSC at one class to deteriorate to the next, as shown in Table 4.

Substituting $n_j S_j^3$ into Eq. (15), the following can be obtained:

$$AFD(t) = \frac{N_p \cdot N_{T1} \cdot FD_1}{A} + \frac{N_p \cdot N_{T2} \cdot FD_2}{A} + \cdots + \frac{N_p \cdot N_{T5} \cdot FD_5}{A} = \frac{\sum_{j=1}^{5} N_p \cdot N_{Tj} \cdot FD_j}{A} \tag{16}$$

After substituting Eq. (16) into Eq. (14), the following can be obtained:

$$g(X) = \Delta - \frac{\sum_{j=1}^{5} N_p \cdot N_{Tj} \cdot FD_j}{A} \tag{17}$$

The statistical properties of the FD_j are summarized in Table 6. The fatigue-strength coefficient A was also found to follow a lognormal distribution with a mean value of 2.57×10^{13} MPa^3 (7.85×10^{10} ksi^3) and a coefficient of variation of 0.35 (Category B) [41].

In the present study, the iterative Rackwitz-Fiessler algorithm was employed to calculate the bridge girder fatigue reliability index based on Eq. (17) [42], and the target reliability index was chosen to be 3.5 as specified in the AASHTO LRFD Bridge Design Specifications [1]. The number of pavement maintenance cycles (N_p) and the total time (T_p) required for fatigue reliability index of the bridge girder to decrease to the target reliability index was obtained and summarized in Table 7. It should be noted that two conditions, namely, Condition "a" and Condition "b", were considered for the pavement life cycle in calculating the fatigue reliability. The only difference between the two conditions is that Condition "a" includes all five RSCs for the pavement life cycle when calculating the fatigue reliability index of the bridge girder using Eq. (17) while Condition "b" does not include the "very poor" RSC. In other words, for Condition "b" it was assumed that maintenance is conducted before the pavement turns into the "very poor" condition. It should also be noted that the pavement deterioration rates and cycles in Table 4 were assumed.

From Table 7, it can be observed that under Condition "b", i.e., if pavement maintenance is conducted regularly before the pave-

Table 7
Number of pavement maintenance, N_p, and the total time in years (T_p) required for the bridge fatigue reliability index to decrease to the target reliability index.

Bridge number	N_p	T_p (years)
1	1[a]|20[b]	24.73|237.20
2	3|15	49.58|180.61
3	19|68	250.76|783.19
4	23|77	289.80|884.73
5	12|14	162.29|170.20

[a] Condition "a": all five RSCs are considered, i.e., very poor, poor, average, good, and very good.
[b] Condition "b": all five RSCs are considered except the "very poor" RSC.

ment turns into very poor condition, the total time required for the fatigue reliability of the bridge girders of all five bridges to decrease to the target reliability index is longer than 75 years, indicating that the fatigue reliability index of all the bridge girders is above 3.5 after 75-year service life. It can also be observed that under Condition "a" the total time required for the fatigue reliability index of the bridge girders of the two shorter bridges to decrease to the target reliability index of 3.5 is significantly less than 75 years, namely, less than 25 years for Bridge 1 and less than 50 years for Bridge 2. This indicates the significant influence of maintaining the pavement condition on increasing the fatigue life and fatigue reliability of steel bridge girders.

Fig. 8(a) plots the variation of the fatigue reliability indexes of all the bridge girders considered against their service time. In order to achieve a better visual effect, only the reliability indexes at the end of each pavement maintenance cycle are plotted in Fig. 8(a) while the elaborated variation of the fatigue reliability indexes of the bridge girders are plotted against their service time, using Bridge 1 as an example, in Fig. 8(b).

From Fig. 8 it can be observed that the fatigue reliability indexes of the bridge girders decrease with the increase of their service time under both conditions. It can also be observed by comparing Condition"a" and Condition "b" that the reliability index of the bridge girders is significantly affected by the very poor RSC. The fatigue reliability indexes of the bridge girders can be reduced by 1 to over 2 for different bridges if the RSC is allowed to deteriorate into the very poor condition. In addition, from Fig. 8(b) it can be seen that the fatigue reliability of bridge girders, during one pavement maintenance cycle, decreases slowly at the beginning until a point when the RSC enters the worst possible condition and the fatigue reliability then drops rapidly. This again indicates that poor RSC has a significant effect on the fatigue reliability index of bridge girders.

In order to meet the target reliability index of 3.5 after 75 years of service for the two shorter bridges considered, based on Eq. (17) it was calculated that the total time that Bridge 1 and Bridge 2 could stay in the class of "very poor" RSC during their 75-year design life should be less than 1.97 and 4.07 years, respectively. This means the pavement maintenance for Bridge 1 and Bridge 2 should be conducted every 11.69 and 12.00 years on average with the number of the pavement maintenance to be six during the 75-year design life. In contrast, the pavement maintenance cycle in some states of the United States is specified longer than the values calculated above. For example, the first and second pavement maintenances of the steel bridges in the state of Indiana are suggested to be conducted after around 20 and 55 years of service, respectively [43]. In addition, it should be noted that nearly fourteen percent of the bridges in the United States are classified as structurally deficient, and many of those bridge decks are in very poor conditions [40].

It should be noted that the results in Table 7 and Fig. 8 were based on the assumed traffic and environmental conditions and the specific bridge considered and were only for the purpose of illustration. In order to account for more general conditions, the following procedure was proposed for determining the pavement maintenance cycle that can meet the target fatigue reliability of the steel girders:

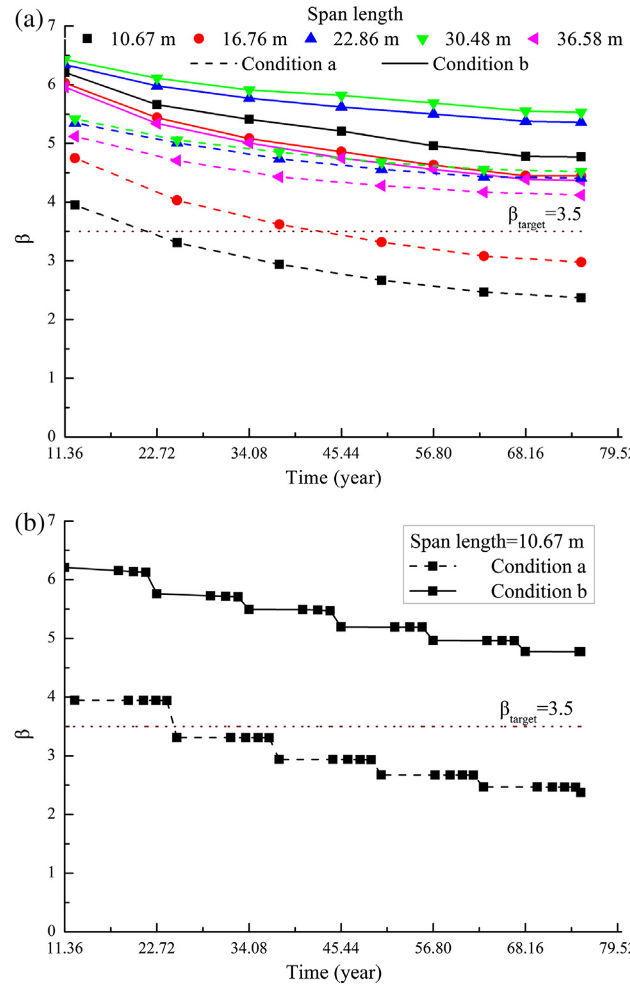

Fig. 8. Variation of the fatigue reliability indexes of all the bridge girders considered against their service time.

(1) based on the environmental condition, calculate the total time that the pavement can stay in each RSC and thus obtain the number of trucks passing the bridge under each RSC based on the ADTT;
(2) obtain the maximum stress range and its *ENSC* of the target point under each *RSC* through a three-dimensional bridge-vehicle interaction analysis and then calculate the *FD* under each RSC and check its distribution pattern;
(3) based on the Miner's rule, the *S-N* curve, and the parameters obtained from the above two steps, an equation similar to Eq. (17) can be obtained and used to determine the pavement maintenance cycle that can meet the target fatigue reliability of the steel girders considered.

8. Summary and conclusion

Deteriorated road surface condition can significantly intensify the vehicle-induced bridge vibration and increase the fatigue damage of bridge components. In this study, the effects of pavement condition on the vehicle-induced fatigue damage and on the fatigue reliability of steel bridge girders were investigated. It was found that the bridge reliability index decreases dramatically when pavement condition gets worse, especially when the pavement is in very poor condition. More specifically, the fatigue reliability index of the bridge girders can be reduced by 1 to over 2 for different bridges if the RSC is allowed to deteriorate into the very poor condition. Therefore, the pavement maintenance cycle has a remarkable influence on the fatigue reliability of the steel girders. A procedure for determining the desired pavement maintenance cycle to achieve the target fatigue reliability of steel bridge girders was put forward. An example was also provided for demonstrating the proposed procedure.

It should be noted that the effect of environmental erosion on the steel fatigue strength was not considered in the fatigue analysis in this research. It should also be noted that a few important parameters, including the traffic condition and environmental condition, have significant influence in the calculation of fatigue reliability of bridge components. In this study, the traffic and environmental condition suggested by the AASHTO LRFD Bridge Design Specifications were adopted for the purpose of illustration. Therefore, more rational assumptions based on field measurement or monitoring data should be adopted when considering a particular field bridge in practice.

Acknowledgments

The authors would like to acknowledge the financial support provided by the National Natural Science Foundation of China (Grant No. 51208189 and No. 51478176) and the Excellent Youth Foundation of Hunan Scientific Committee (Grant No. 14JJ1014).

References

[1] AASHTO. AASHTO LRFD bridge design specifications. 6th ed. AASHTO. Washington, D.C.; 2012.
[2] Zhang W, Cai C. Fatigue reliability assessment for existing bridges considering vehicle speed and road surface conditions. J Bridge Eng 2012;17:443–53.
[3] Zhang W, Cai C. Reliability-based dynamic amplification factor on stress ranges for fatigue design of existing bridges. J Bridge Eng 2013;18:538–52.
[4] Abaza KA. Optimum flexible pavement life-cycle analysis model. J Transport Eng 2002;128:542–9.
[5] Labi S, Sinha KC. Life-cycle evaluation of flexible pavement preventive maintenance. J Transport Eng 2005;131:744–51.
[6] Chan A, Keoleian G, Gabler E. Evaluation of life-cycle cost analysis practices used by the Michigan Department of Transportation. J Transport Eng 2008;134:236–45.
[7] Santos J, Ferreira A. Pavement design optimization considering costs and preventive interventions. J Transport Eng 2011;138:911–23.
[8] Gransberg DD, Molenaar KR. Life-cycle cost award algorithms for design/build highway pavement projects. J Infrastruct Syst 2004;10:167–75.
[9] Li Z, Madanu S. Highway project level life-cycle benefit/cost analysis under certainty, risk, and uncertainty: methodology with case study. J Transport Eng 2009;135:516–26.
[10] Rajbongshi P, Das A. Optimal asphalt pavement design considering cost and reliability. J Transport Eng 2008;134:255–61.
[11] Sanchez-Silva M, Arroyo O, Junca M, Caro S, Caicedo B. Reliability based design optimization of asphalt pavements. Int J Pavement Eng 2005;6:281–94.
[12] Deshpande VP, Damnjanovic ID, Gardoni P. Reliability-based optimization models for scheduling pavement rehabilitation. Comput-Aided Civil Infrastruct Eng 2010;25:227–37.
[13] ANSYS 14.5 [Computer software]. Canonsburg P, Ansys.
[14] Shi XM, Cai CS, Chen SR. Vehicle induced dynamic behavior of short-span slab bridges considering effect of approach slab condition. J Bridge Eng 2008;13:83–92.
[15] Chotickai P, Bowman M. Truck models for improved fatigue life predictions of steel bridges. J Bridge Eng 2006;11:71–80.
[16] Snyder RE, Likins GE, Moses F. Loading spectrum experienced by bridge structures in the United States Report No. FHWA/RD-85/012. Warrensville, Ohio: Bridge Weighing Systems Inc.; 1985.
[17] Deng L, Cai CS. Identification of dynamic vehicular axle loads: theory and simulations. J Vib Control 2010;16:2167–94.
[18] Deng L, Cai CS. Development of dynamic impact factor for performance evaluation of existing multi-girder concrete bridges. Eng Struct 2010;32:21–31.
[19] Deng L, Cai C. Bridge model updating using response surface method and genetic algorithm. J Bridge Eng 2009;15:553–64.
[20] Deng L, Cai CS. Identification of dynamic vehicular axle loads: demonstration by a field study. J Vib Control 2011;17:183–95.
[21] Dodds C, Robson J. The description of road surface roughness. J Sound Vib 1973;31:175–83.
[22] Huang D, Wang T-L. Impact analysis of cable-stayed bridges. Comput Struct 1992;43:897–908.
[23] ISO. Mechanical vibration-road surface profiles-reporting of measured data. ISO 8068: (E), Geneva; 1995.
[24] Wang W, Deng L, Shao X. Number of stress cycles for fatigue design of simply-supported steel I-girder bridges considering the dynamic effect of vehicle loading. Eng Struct 2016;110:70–8.
[25] Shiyab A. Optimum use of the flexible pavement condition indicators in pavement management system [Ph.D Thesis]. Perth, Australia: Curtin University of Technology; 2007.
[26] Chang D, Lee H. Impact factors for simple-span highway girder bridges. J Struct Eng 1994;120:704–15.
[27] Liu C, Huang D, Wang T-L. Analytical dynamic impact study based on correlated road roughness. Comput Struct 2002;80:1639–50.
[28] Yang Y-B, Liao S-S, Lin B-H. Impact formulas for vehicles moving over simple and continuous beams. J Struct Eng 1995;121:1644–50.
[29] Miner MA. Cumulative damage in fatigue. J Appl Mech 1945;12:159–64.
[30] Albrecht P, Friedland IM. Fatigue-limit effect on variable-amplitude fatigue of stiffeners. J Struct Divis 1979;105:2657–75.
[31] Schilling CG, Klippstein KH, Barsom JM, Blake GT. Fatigue of welded steel bridge members under variable-amplitude loadings NCHRP Rep 188. Washington, D.C: Transportation Research Board; 1978.
[32] Keating PB, Fisher JW. Review of fatigue tests and design criteria on welded details Fritz Engineering Laboratory Report 488-1(85). Bethlehem, Penn: Lehigh University; 1986.
[33] Schilling C. Stress cycles for fatigue design of steel bridges. J Struct Eng 1984;110:1222–34.
[34] Schilling C. Impact factors for fatigue design. J Struct Divis 1982;108:2034–44.
[35] Connor RJ, Fisher JW, Hodgson IC, Bowman CA. Results of field monitoring prototype floorbeam connection retrofit details on the Birmingham Bridge. Bethlehem (PA): Lehigh University's Center for Advanced Technology for Large Structural Systems (ATLSS); 2004.
[36] Connor R, Hodgson I, Mahmoud H, Bowman C. Field testing and fatigue evaluation of the I-79 Neville Island Bridge over the Ohio River. Bethlehem (PA): Lehigh University's Center for Advanced Technology for Large Structural Systems (ATLSS); 2005.
[37] Kwon K, Frangopol DM. Bridge fatigue reliability assessment using probability density functions of equivalent stress range based on field monitoring data. Int J Fatigue 2010;32:1221–32.
[38] Liu M, Frangopol DM, Kwon K. Fatigue reliability assessment of retrofitted steel bridges integrating monitored data. Struct Saf 2010;32:77–89.
[39] Brady SP, O'Brien EJ, Žnidarič A. Effect of vehicle velocity on the dynamic amplification of a vehicle crossing a simply supported bridge. J Bridge Eng 2006;11:241–9.
[40] Robelin C-A, Madanat SM. History-dependent bridge deck maintenance and replacement optimization with Markov decision processes. J Infrastruct Syst 2007;13:195–201.
[41] Chung H-Y. Fatigue reliability and optimal inspection strategies for steel bridges [Ph.D]. Texas: University of Texas at Austins; 2004.
[42] Nowak AS, Collins KR. Reliability of structures. CRC Press; 2012.
[43] Cha H, Liu B, Prakash A, Varma AH. Effect of local damage caused by overweight trucks on the durability of steel bridges. J Perform Constr Facil 2014;30:1–11.